In situ complexation versus complex isolation in synthesis of ion imprinted polymers

Katri Laatikainen, Catherine Branger, Bruno Coulomb, Véronique Lenoble, Tuomo Sainio

Reactive and Functional Polymers 122 (2018) 1–8

Contents lists available at ScienceDirect

Reactive and Functional Polymers

journal homepage: www.elsevier.com/locate/react

In situ complexation *versus* complex isolation in synthesis of ion imprinted polymers

Katri Laatikainen[a,*], Catherine Branger[b], Bruno Coulomb[c], Véronique Lenoble[d], Tuomo Sainio[a]

[a] Lappeenranta University of Technology, Laboratory of Separation Technology, P.O. Box 20, FI-53851 Lappeenranta, Finland
[b] University of Toulon, MAPIEM, EA 4323, CS 60584, 83041 Toulon, Cedex 9, France
[c] Aix-Marseille Univ, CNRS, LCE, Marseille, France
[d] University of Toulon, PROTEE, EA 3819, CS 60584, 83041 Toulon, Cedex 9, France

ARTICLE INFO

Keywords:
N-(4-vinylbenzyl)-2-(aminomethyl)pyridine (Vbamp)
Nickel
Distribution of complexes
Isolation of complexes
Ion imprinted polymers (IIP)

ABSTRACT

In this study, the object is to prove that isolation of complexes made by varying the metal/ligand ratio (*in situ* complexation) yields similar polymer characteristics, metal binding and selectivity results as polymers synthesized by isolating the complex by precipitation. Complexation between nickel and the *N*-(4-vinylbenzyl)-2-(aminomethyl)pyridine (Vbamp) monomer was studied in dimethyl sulfoxide (DMSO) and in a DMSO-methanol mixture (50:50, v/v) at 80 °C using a $Ni(NO_3)_2{\cdot}6H_2O$ salt as the nickel source. According to the results, the three nickel/Vbamp complexes could be selectively obtained using specific conditions: for $[Ni(Vbamp)]^{2+}$ the Ni/Vbamp ratio in DMSO was 1.08, for $[Ni(Vbamp)_2]^{2+}$ the Ni/Vbamp ratio DMSO-methanol (50:50, v/v) was 0.49 and for $[Ni(Vbamp)_3]^{2+}$ the Ni/Vbamp ratio in DMSO was 0.3. Ion-imprinted polymers (IIPs) were prepared either with $[Ni(Vbamp)](NO_3)_2$, $[Ni(Vbamp)_2](NO_3)_2$, or $[Ni(Vbamp)_3](NO_3)_2$ complexes as the template. IIP with a $[Ni(Vbamp)_3]^{2+}$ complex, isolated by precipitation prior to polymerization, was also prepared. The results demonstrated that surface properties, nickel binding and selectivity properties were similar for both kind of IIPs – prepared by *in situ* complexation or isolation of the complex prior to polymer synthesis. Selectivity coefficients of nickel toward zinc for IIPs with $[Ni(Vbamp)]^{2+}$, $[Ni(Vbamp)_2]^{2+}$ and $[Ni(Vbamp)_3]^{2+}$ templates were close to 1038, 1441 and 1463, respectively.

1. Introduction

In the search for highly selective separation sorbents, ion imprinting technique leads to very attractive materials [1]. Their remarkable recognition properties come from their method of preparation. Synthesis of ion imprinted polymers usually consists of three steps: complexation between a polymerizable ligand and the template metal ion, copolymerization of the complex with a matrix-forming monomer and removal of the metal ion after polymerization [2]. The selectivity of the formed ion-imprinted polymers (IIPs) depends on the stability of the complex and on the size and shape of the generated cavities [3]. For the separation of transition metals, IIPs are usually based on chelating ligands, because of their ability to form strong coordinative bonds with metal cations [4]. In the development of ion imprinted materials, the challenge is still to prepare highly selective materials, which efficiently work in actual process conditions. Thus, new ideas improving the synthesis and selectivity of IIPs are still needed [5].

In the synthesis of IIPs, isolation of ligand-metal complexes has been extensively studied [6–13]. Isolation of complexes can be accomplished by crystallization of the complex in a separate step and re-dissolution in the polymerization mixture [6–13]. Crystallization of the complex is a reliable but time-consuming way to isolate the desired structure. Moreover, the back-dissolution step in the polymerization medium is often problematic. An alternative, simple and quick procedure is to form the complex directly in the pre-polymerization medium by mixing the metal and the ligand in a well-defined metal/ligand ratio [14–21]. In this case, the stoichiometry of the complex before polymerization is commonly checked by absorbance spectroscopy [15–18,20–22]. When only one structure of the complex is formed, as in the case of the 1-hydroxy 2-(prop-2′-enyl)-9,10-anthraquinone ligand and uranyl, this method is suitable [20]. However, when multiple complexes form, overlapping spectra are obtained and specific methods are required to determine the distribution of the various complexes. Continuous variation analysis originally introduced by Job [23] and ligand titration are normally used to analyze the spectral data [15,18,21]. However, these are only approximate methods and in the case of more complicated systems, the exact distribution of the complexes in the pre-polymerization medium usually remains unclear. Least-squares

* Corresponding author.
E-mail address: Katri.Laatikainen@lut.fi (K. Laatikainen).

https://doi.org/10.1016/j.reactfunctpolym.2017.10.022
Received 19 April 2017; Received in revised form 27 October 2017; Accepted 30 October 2017
Available online 31 October 2017

minimization [24] enables calculation of the distribution of the complexes from the spectral data [25–26]. Despite its efficiency, apart from our team [25–26], only Shamsipur et al. [16–17] have implemented non-linear fitting of spectral data for determination of the distribution of complexes before the synthesis of IIPs.

The aim of this study is to prove that isolation of complexes made by varying the metal/ligand ratio and solvent mixture at 80 °C in the pre-polymerization medium (*in situ* complexation) yields similar polymer characteristics, metal binding and selectivity results as polymers made by isolating the complex by crystallization. *In situ* complexation method represents a simple way to control the stoichiometry of Ni/Vbamp complexes, while avoiding a conventional isolation method (crystallization or precipitation). In order to validate the efficiency of this new synthetic route, nickel uptake capacities and nickel/zinc selectivity of the IIPs were compared with those of an IIP prepared from a $[Ni(Vbamp)_3]^{2+}$ complex, which was isolated *via* prior polymerization [27]. Furthermore, to the best of our knowledge, no studies concerning IIPs with different stoichiometries between the specific ligand and the metal can be found in the literature. It is noteworthy that there are many excellent papers published recently in which high selective have been achieved, but complex formation study have been ignored although it is presumable that different complex stoichiometries can be formed [28–30]. In this study, we show the effect of the stoichiometry of the complex on material characteristics, metal binding and selectivity properties.

The *N*-(4-vinylbenzyl)-2-(aminomethyl)pyridine (Vbamp) monomer was chosen for this study, because of the ability of the 2-(aminomethyl) pyridine ligand to form three different complexes with nickel and its stability constants for high Ni/Zn selectivity are promising [31]. Complexation between nickel and Vbamp was studied by recording absorbance spectra with different nickel/Vbamp ratios and solvent compositions (dimethyl sulfoxide (DMSO), or a mixture of DMSO and methanol (50:50, v/v)) at 80 °C. The distribution of the complexes was obtained by analyzing the spectral data using a least-squared minimization scheme [24–25]. Subsequently, IIPs with three different structures ($[Ni(Vbamp)](NO_3)_2$, $[Ni(Vbamp)_2](NO_3)_2$ and $[Ni(Vbamp)_3](NO_3)_2$) were prepared by inverse suspension polymerization using ethylene glycol dimethacrylate (EDMA) as the crosslinking agent.

2. Experimental

2.1. Materials and instrumentation

2-(aminomethyl)pyridine (2-picolylamine, 99%, Sigma-Aldrich), 3-vinylbenzaldehyde (97%, Sigma-Aldrich), $NaBH_4$ (99.99%, Sigma-Aldrich), toluene (99.9%, Sigma-Aldrich), ethanol (99.8%, Fluka), diethyl ether (99.9%, inhibitor free, Sigma-Aldrich) and $MgSO_4$ (99.5%, anhydrous, Sigma-Aldrich) were reagent grade chemicals used without further purification. Methanol (99.9%, Sigma-Aldrich), DMSO (99.9% Sigma-Aldrich), $Ni(NO_3)_2{\cdot}6H_2O$ (98.5%, Sigma-Aldrich), $NiSO_4{\cdot}6H_2O$ (99%, Fluka), and $Na_2SO_4{\cdot}10H_2O$ (99%, Sigma-Aldrich), were used in experiments to form the complexes. Mineral oil (heavy, Sigma-Aldrich), 2,2′-azobisisobutyrontrile (AIBN) (98%, Sigma-Aldrich) and EDMA (98%, Acros) used in the polymerization was washed with a solution of 10% NaOH (99.9%, Sigma-Aldrich), dried on $MgSO_4$ and distilled to remove inhibitors. Aqueous solutions were prepared using deionized water (conductivity less than 0.1 μS cm^{-1}).

Absorbance spectra of the nickel and Vbamp complexes were measured with a UV–vis spectrophotometer (Jasco V670) using a quartz cuvette with a light path of 1 cm. The concentrations of the sample solutions are estimated to be correct within 2%. The accuracy of the spectra was tested by repeating a measurement four times over a period of 4 h. The average absolute difference in the wavelength range 400–1000 nm was 0.001 absorbance unit.

Structures of the nickel and Vbamp complexes after polymerization of IIPs were analyzed using a reflection UV–vis-NIR spectrophotometer (JASCO V670) equipped with a horizontal integrating sphere attachment (JASCO PIN-757). Spectra were measured between 190 and 1000 nm with a 400 nm·min^{-1} scan speed using the corresponding non-imprinted polymers (NIPs) as a reference.

FTIR spectra were obtained using the standard KBr pellet method (Perkin–Elmer Frontier FTIR). The number of scans was 64 and the resolution was 4 cm^{-1}.

The BET surface area, BJH pore volume and pore size were measured using N_2 adsorption (Micromeritics Gemini V). Nitrogen adsorption/desorption isotherms were also measured. Before the measurements were collected, samples were evacuated several hours at a pressure less than 10^{-3} Pa at 50 °C. The shape of the particles was analyzed using scanning electron microscopy (SEM, JEOL JSM-5800).

Metal concentrations were determined by inductively coupled plasma-atomic emission spectroscopy on a ICP-AES (Iris Intrepid IIXDL ICP-AES). All samples were analyzed at least twice and the duplicate determinations agreed within 5%.

2.2. Complexation of nickel with the 2-(aminomethyl)pyridine monomer

The functional monomer, *N*-(4-vinylbenzyl)-2-(aminomethyl)pyridine (Vbamp) was synthesized *via* Schiff base reaction and subsequent reduction of the imine as previously described [26]. The complexation between nickel and Vbamp was studied in DMSO and a DMSO/methanol mixture (50:50, v/v) using $Ni(NO_3)_2{\cdot}6H_2O$ as the nickel source. The procedure is illustrated in Scheme 1. The experiments were performed in 3 mL glass vials. The combined concentration of the nickel (0.01–0.09 mol L^{-1}) and Vbamp (0.09–0.01 mol L^{-1}) was kept constant (0.1 mol L^{-1}), but the mole ratio of the ligand and metal was varied. Typically, 14 spectra at different mole ratios were recorded. The spectra were recorded at 80 °C using a UV–vis spectrophotometer.

At equilibrium, the distribution of the complexes was calculated using a commercial program (HypSpec) based on the least-squares minimization scheme [24]. Stability constants, extinction coefficients, and concentrations of all absorbing components were simultaneously estimated. For uncomplexed nickel, the extinction coefficients were known from independent measurements. Detailed description of the calculations can be found in our previous paper [25].

2.3. Synthesis of ion-imprinted polymers

Each complex was copolymerized with EDMA crosslinker to prepare IIP1a, IIP1b and IIP1c (with $[Ni(Vbamp)](NO_3)_2$), IIP2 (with $[Ni(Vbamp)_2](NO_3)_2$) and IIP3 (with $[Ni(Vbamp)_3](NO_3)_2$) by inverse suspension copolymerization. Solutions containing predominantly the complexes with 1:1, 1:2 and 1:3 stoichiometries were prepared from Ni/Vbamp molar ratios of 1.1, 1.5 and 4.0 for $[Ni(Vbamp)](NO_3)_2$, 0.5 for $[Ni(Vbamp)_2](NO_3)_2$ and 0.3 for $[Ni(Vbamp)_3](NO_3)_2$ (Table 1). The solvents were respectively, DMSO, a DMSO-methanol mixture (50:50, v/v) and DMSO. The volume of the solvent was 10 mL, the mass of Vbamp was kept constant at 0.519 g (0.002 mol) and $Ni(NO_3)_2{\cdot}6H_2O$ was used as the nickel source (the amount was calculated from the Ni/Vbamp mole ratios). In the case of IIP4, $Ni(Vbamp)_3(ClO_4)_2$ complex was precipitated by slow evaporation after one day according to Lenoble et al. [27]. Additionally, 4.4 mL (0.02 mol) of EDMA and 0.1 g of AIBN were added, to the solution and stirring under nitrogen was maintained for 15 min. 80 mL of mineral oil was introduced in a 500 mL round-bottom flask and purged with nitrogen for 15 min. The organic phase containing the monomers and AIBN was then added quickly. Polymerization was performed at 80 °C for 4 h under nitrogen with stirring rates of 1000 rpm (IIP1a, IIP1b, IIP1c and IIP2), 250 rpm (IIP3) and 750 rpm (IIP4). The polymer particles formed were filtered, washed with 50 mL chloroform and extracted in a Soxhlet tube for 24 h with a chloroform-acetone mixture (1:1). Finally, the particles were dried under vacuum at 25 °C for 24 h. NIPs were prepared in DMSO (NIP1) and in the DMSO-methanol mixture (50:50, v/v) (NIP2) under

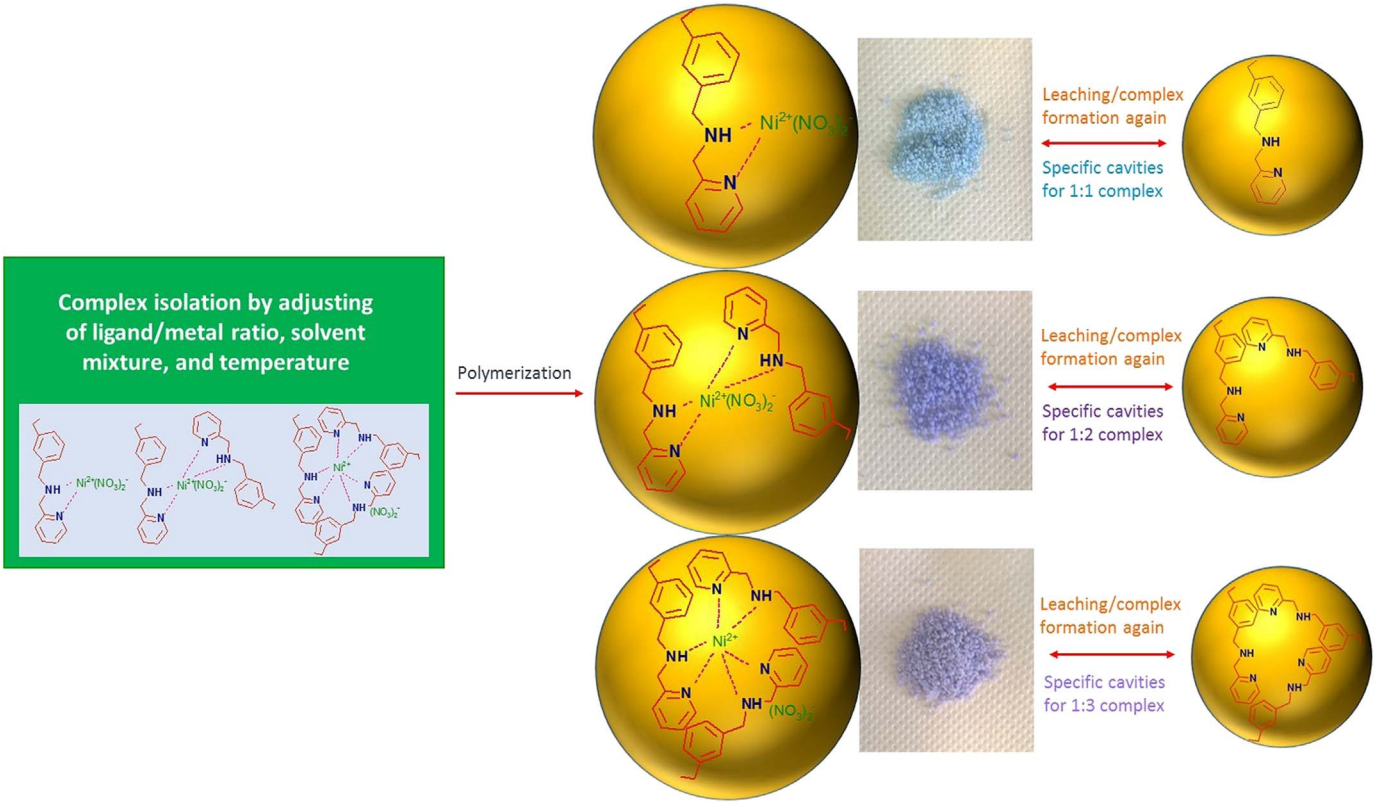

Scheme 1. Adjustment of the nickel complex structure with the Vbamp monomer in different solvent mixtures.

Table 1
Conditions of preparation of the IIPs with mole fractions determined at 80 °C.

Polymer	Major complex	Solvent	Ni/Vbamp mole ratio	$x_{1:1}$, %[a]	$x_{1:2}$, %[a]	$x_{1:3}$, %[a]	x_{Ni}, %[b]	$x_{Vbamp,\ \%}$[c]
IIP1a	$[Ni(Vbamp)]^{2+}$	DMSO	1.1	97	0	3	9	0
IIP1b	$[Ni(Vbamp)]^{2+}$	DMSO	1.5	99	1	0	33	0
IIP1c	$[Ni(Vbamp)]^{2+}$	DMSO	4.0	100	0	0	76	0
IIP2	$[Ni(Vbamp)_2]^{2+}$	DMSO and methanol (50:50, v/v)	0.5	3	95	2	0	0
IIP3	$[Ni(Vbamp)_3]^{2+}$	DMSO	0.30	0.0	6	94	0	6

[a] $x_{1:i}$ represents the mole fraction of the complex of 1:i stoichiometry relative to the total amount of the three complexes.
[b] x_{Ni} represents the mole fraction of nickel relative to the total amount of introduced nickel.
[c] x_{Vbamp} represents the mole fraction of Vbamp relative to the total amount of introduced Vbamp.

identical conditions (with 0.519 g of Vbamp), except for the omission of nickel.

The nickel template was removed from the IIPs by treating 0.01 g of each with 10 mL of 5 M H_2SO_4 for 2 h with shaking. Subsequently, the H_2SO_4 solution was separated from the polymer and analyzed by ICP-AES.

2.4. Characterization of IIPs

Before removing nickel from the polymer, the nickel-Vbamp complex structures formed in the IIPs were analyzed using the reflection UV–vis-NIR spectrophotometer.

Regeneration of the IIPs was studied using FTIR spectroscopy. The shapes of the particles were analyzed using scanning electron microscopy.

BET surface areas, BJH pore volumes and average pore sizes were measured using nitrogen adsorption/desorption experiments.

2.5. Metal binding properties of IIPs

Before metal binding tests, the polymers were treated in a glass column consecutively with 5 bed volumes (BVs) of 5 M H_2SO_4, 5 BVs of water, 5 BVs of 1 M NaOH and 5 BVs of water. The cycle was repeated three times. Finally, the polymers were rinsed copiously with water and subsequently dried under vacuum at 25 °C for 24 h.

Nickel binding measurements were conducted from pure nickel sulphate solution (initial concentration 2.5 mmol·L^{-1}) and from a mixture of nickel and zinc sulphate (initial concentrations for nickel and zinc were 0.3 and 300 mmol·L^{-1}, respectively) at room temperature (22–24 °C) at pH 4. 0.01 g of the polymer was weighed in a plastic tube containing the nickel sulphate solution. The liquid volume of all samples was 10 mL. The bottles were shaken at room temperature for 7 days. The pH of the samples was kept constant by addition of sulfuric acid or sodium hydroxide. Then, the metals were leached out from the polymers with 10 mL of 5 M H_2SO_4. The bound amounts were calculated from the analyses of the desorption solution. Metal concentrations were determined by ICP-AES. The values are given per unit weight of dry base-form adsorbent. Imprinting factors and selectivity coefficients, k, for binding of specific metal ions in the presence of competitor species can be obtained from the adsorption data according to Eqs. (1), (2) and (3) [32], in which q and c are the metal binding capacity (mmol·g^{-1}) and the concentration (mol·L^{-1}), respectively.

$$\text{Imprinting factor} = \frac{q_{Ni,IIP}}{q_{Ni,NIP}} \quad (1)$$

$$k_{Zn}^{Ni} = \frac{q_{Ni} c_{Zn}}{q_{Zn} c_{Ni}} \quad (2)$$

The effect of ion imprinting on selectivity was quantified by calculating relative selectivity coefficient, k', defined in Eq. (4) [32]; k_{IIP} and k_{NIP} are the selectivity coefficients of imprinted and non-imprinted polymers, respectively.

$$k' = \frac{k_{IIP}}{k_{NIP}} \quad (3)$$

3. Results and discussion

3.1. Distributions of complexes obtained by adjustment of metal/ligand ratio and solvent

In order to control the stoichiometry of nickel complexes with Vbamp before the synthesis of IIPs, the distribution of the complexes was determined by analyzing the absorbance spectra recorded in DMSO and in the DMSO-methanol mixture (50:50, v/v). The measurements were made at 25 and 80 °C, but the results are shown only at 80 °C, because that was the polymerization temperature. The Ni/Vbamp ratio was varied from 0.1 to 5.3 using $Ni(NO_3)_2{\cdot}6H_2O$ as the nickel source. The distribution curves of the complexes are depicted in Fig. 1 and the fraction of each complex used to prepare the IIPs are given in Table 1.

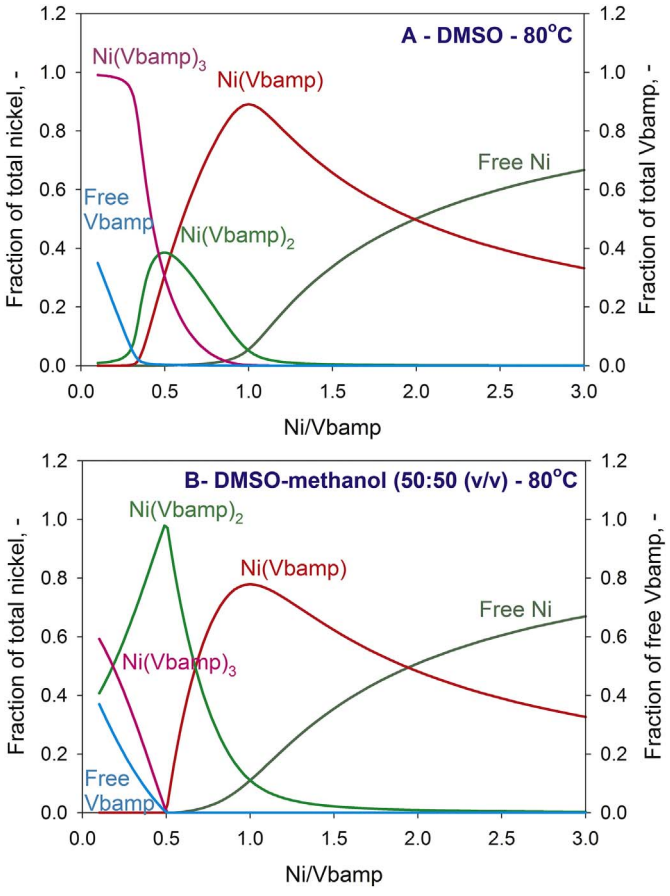

Fig. 1. Distributions of complexes calculated from UV–vis spectra using the HypSpec program [Gans] between nickel and Vbamp at different Ni/Vbamp ratios using Ni $(NO_3)_2{\cdot}6H_2O$ as the nickel source at 80 °C. Solvent: (A) DMSO and (B) DMSO-methanol mixture (50:50, v/v).

Table 2
Step-wise stability constants of log$K$ for $[Ni(Vbamp)]^{2+}$, $[Ni(Vbamp)_2]^{2+}$, and $[Ni(Vbamp)_3]^{2+}$ in the solvent mixtures at 25 and 80 °C.

Temperature	25 °C			80 °C		
Solvent	logK_1	logK_2	logK_3	logK_1	logK_2	logK_3
DMSO	5.41	4.14	2.95	6.16	3.70	3.51
DMSO and methanol (50:50, v/v)	7.26	4.65	3.66	5.95	4.58	1.20

The amount of each complex is given as mole fractions of the total distribution. The amount of uncomplexed nickel and Vbamp are also given as mole fractions relative to their total concentrations. When the Ni/Vbamp mole ratio is very low, uncomplexed Vbamp existed in the solution, which did not take part in the complexation reactions. The presence of uncomplexed Vbamp monomer will disturb the ion-imprinting effect because, during the polymerization, it will generate binding sites that are analogous to the sites of NIPs. However, as shown in our previous study, uncomplexed Vbamp below 10% does not significantly affect the selectivity properties of the IIPs [26]. As observed in Table 1, in the cases of IIP1a–IIPc, uncomplexed nickel existed in the pre-polymerization solution. The impact of such uncomplexed Ni on the corresponding IIP characteristics and nickel binding selectivity properties is also further studied.

Step-wise stability constants are shown in Table 2 at 25 and 80 °C in DMSO and DMSO-methanol (50:50, v/v mixture). According to the results, by increasing the temperature from 25 to 80 °C, the selective formation of the complexes improved. In DMSO, as the temperature increased, the values for logK_1 and logK_3 increased, whereas logK_2 decreased slightly. In the DMSO-methanol (50:50, v/v) mixture, logK_1 and logK_3 decreased and logK_2 remained almost unchanged. Furthermore, it can be observed from Table 2 that by mixing methanol with DMSO at 80 °C, the stability constant, logK_2, of the $[Ni(Vbamp)_2]^{2+}$ complex increased and logK_1 and logK_3 decreased compared to constants measured in pure DMSO. The formation of the $[Ni(Vbamp)_2]^{2+}$ complex in the DMSO-methanol mixture was favored by increasing its domain of stability. The $[Ni(amp)_2(NO_3)_2]$ complex can be crystallized in water or in water-methanol mixture by mixing 1 equiv. of Ni $(NO_3)_2{\cdot}6H_2O$ with 2 equiv. of amp [33]. In the case of nickel and the Vbamp monomer, although the equilibria are shifted toward the formation of the $[Ni(Vbamp)_2]^{2+}$ complex in the mixture of DMSO-methanol (50:50, v/v), no isolation of this complex could be achieved either by crystallization nor by precipitation. Therefore, the approach consisting of preparing the complex with the desired stoichiometry by controlling the Ni/Vbamp mole ratio in the pre-polymerization medium is a real improvement, because it allows an IIP to be prepared with the 1:2 stoichiometry having a 0.5 Ni/Vbamp ratio in the DMSO-methanol mixture (Table 1).

As can be observed from Fig. 1 and from Table 1, conditions can be found in which only one of the Ni/Vbamp complexes ($[Ni(Vbamp)_3]^{2+}$, $[Ni(Vbamp)_2]^{2+}$, or $[Ni(Vbamp)]^{2+}$) is predominantly present in the solution. The $[Ni(Vbamp)_3]^{2+}$ and $[Ni(Vbamp)]^{2+}$ complexes can be selectively formed in DMSO, whereas selective formation of the $[Ni(Vbamp)_2]^{2+}$ complex requires a DMSO-methanol mixture (50:50, *v*/v) as the solvent. The $[Ni(Vbamp)_2]^{2+}$ complex cannot be formed selectively in DMSO. With the Ni/Vbamp ratio = 0.5 in DMSO (Fig. 1A), the distributions for $[Ni(Vbamp)_3]^{2+}$, $[Ni(Vbamp)_2]^{2+}$, $[Ni(Vbamp)]^{2+}$, uncomplexed Vbamp and nickel are 15, 66, 18, 0 and 0%, respectively.

In conclusion, the $[Ni(Vbamp)]^{2+}$ complex can be selectively formed in DMSO when uncomplexed nickel is introduced in excess (Fig. 1A and Table 1). With Ni/Vbamp ratios of 1.1 (IIP1a), 1.5 (IIP1b) and 4.0 (IIP1c), respectively, 9, 33 and 76% of uncomplexed nickel remained in the solution (Table 1). In the case of the selective formation of the $Ni(Vbamp)_3$ complex in DMSO, 6% of uncomplexed Vbamp was present in the solution (Table 1).

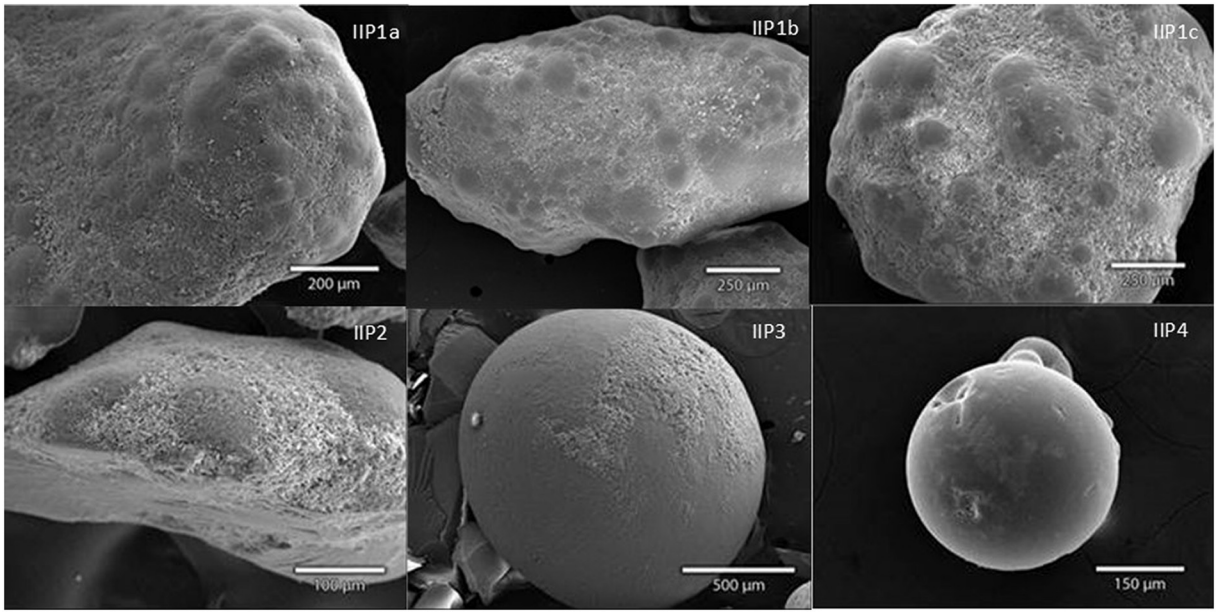

Fig. 2. SEM images of IIPs.

3.2. Synthesis and characterization of IIPs

The previously prepared solutions of $[Ni(Vbamp)]^{2+}$, $[Ni(Vbamp)_2]^{2+}$ and $[Ni(Vbamp)_3]^{2+}$ were used as template sources to prepare nickel IIPs with EDMA as the crosslinking agent. Inverse suspension copolymerization in mineral oil was performed according to a previously described procedure [26,34]. DMSO and the mixture of DMSO-methanol (50:50, v/v) played the role of the porogen agent. Three IIPs (IIP1a, IIP1b and IIP1c) with the $[Ni(Vbamp)]^{2+}$ template were prepared from Ni/Vbamp ratios of 1.1, 1.5 and 4.0. IIP2 and IIP3 involved the $[Ni(Vbamp)_2]^{2+}$ and $[Ni(Vbamp)_3]^{2+}$ complexes, respectively. Two control polymers were synthesized: NIP1 was prepared in DMSO as a reference material for the IIP1s and IIP3 and NIP2 in the DMSO-methanol mixture as a reference material for IIP2. Scanning electron microscopy observations revealed that all polymers were obtained in the form of independent particles with diameters of 600 ± 30 and 400 ± 30 µm for NIP1 and NIP2, respectively. The particle diameters of IIP1a, IIP1b, IIP1c, IIP2, IIP3 and IIP4 were 1500 ± 30, 1500 ± 30, 1500 ± 30, 750 ± 30, 1500 ± 30 and 350 ± 30 µm, respectively (Fig. 2).

In order to evaluate the impact of the preparation of the Ni-Vbamp complex *in situ* in the pre-polymerization medium on the IIPs properties, direct isolation prior to polymerization of the three complexes was tested. Only the $[Ni(Vbamp)_3](ClO_4)_2$ complex could be independently prepared and used to synthesize of IIP4 [31].

The complexes structures inside the IIPs were analyzed by reflection UV–vis spectroscopy. Reflection UV–vis spectra of IIPs 1–4 after polymerization and Soxhlet-extraction, but prior to nickel removal, are illustrated in Fig. 3. The spectrum of the $[Ni(Vbamp)_3](ClO_4)_2$ complex obtained by precipitation is included for comparison. It is clear that the $[Ni(Vbamp)_3]^{2+}$ complex was successfully incorporated into the polymers both by the conventional complex isolation method (IIP4) and by the method proposed in this study (IIP3). The absorption maxima for IIP3 and IIP4 coincide at 578 nm. Furthermore, the absorption maxima of IIP3 and IIP4 are very close to the absorption maximum of the precipitated $[Ni(Vbamp)_3](ClO_4)_2$complex located at 574 nm. Moreover, the absorption bands at higher wavelengths (800–1000 nm) are similar in all three cases.

The absorption maxima for IIP1a, IIP1b and IIP1c are all located at 608 nm (Fig.3), indicating that the structure of the complexes in the polymers is similar. However, the maximum absorption was expected to

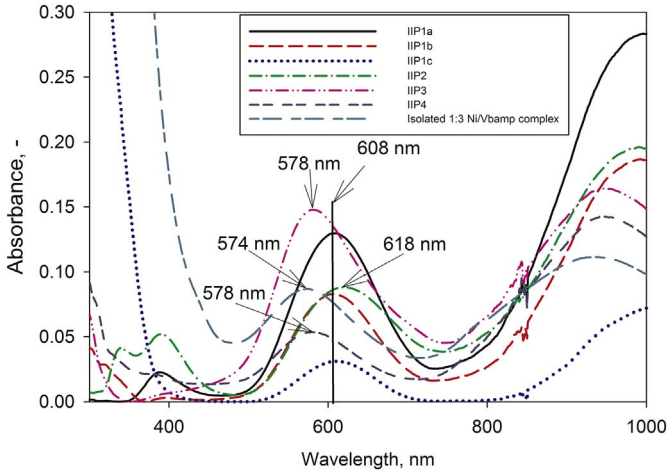

Fig. 3. Reflection UV–vis spectra of IIP1a, IIP1b, IIP1c, IIP2, IIP3, and IIP4 after polymerization and soxhlet-extraction and that of an isolated $[Ni(Vbamp)_3](ClO_4)_2$ complex. Data for IIP4 and the isolated $[Ni(Vbamp)_3](ClO_4)_2$ complex were taken from Lenoble et al. [27].

be located at much higher wavelength. Indeed, from the calculation of the extinction coefficients for $[Ni(Vbamp)](NO_3)_2$, $[Ni(Vbamp)_2](NO_3)_2$ and $[Ni(Vbamp)_3](NO_3)_2$ in DMSO and the DMSO-methanol (50:50, v/v) mixture using the HypSpec program, the absorption maximum for $[Ni(Vbamp)](NO_3)_2$ in DMSO was located at 652 nm (Fig. 4). However, as was illustrated in Table 1, the IIP1c complex was synthesized with a particularly high Ni/Vbamp ratio (4) and it is unlikely that a complex other than $[Ni(Vbamp)](NO_3)_2$ could be formed with such a high surplus of uncomplexed nickel in the solution. Absorption maximum for IIP2 is at 618 nm, which is slightly higher than that observed for $[Ni(Vbamp)_2](NO_3)_2$, using the HypSpec program in Fig. 3 at 600 nm. Anyway, this difference is not so important and might be explained by the difference in the local environment of the complex. Indeed, UV–vis absorption of organic molecules or organometallic complexes is well-known to be very dependent of solvent effects and in the present case, the reflection UV–vis spectra of IIPs were measured on dried polymers whereas UV–vis spectra of the $[Ni(Vbamp)_2](NO_3)_2$ complex was measured in highly-polar solvents.

According to our previous study, nickel can be fully desorbed by

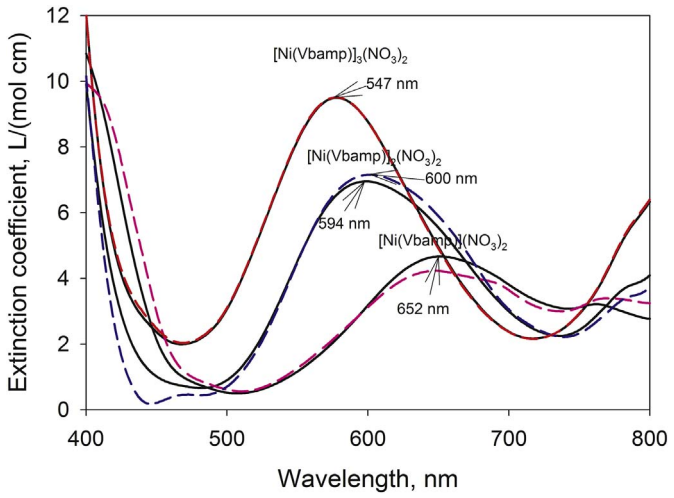

Fig. 4. Extinction coefficients of [Ni(Vbamp)](NO$_3$)$_2$, [Ni(Vbamp)$_2$](NO$_3$)$_2$, and [Ni(Vbamp)$_3$](NO$_3$)$_2$ obtained using the HypSpec program [23–24]. I_s = 0, T = 25 °C, in nitrate media and in DMSO (solid lines) and in the DMSO-methanol (50:50, v/v) (dashed lines) mixture.

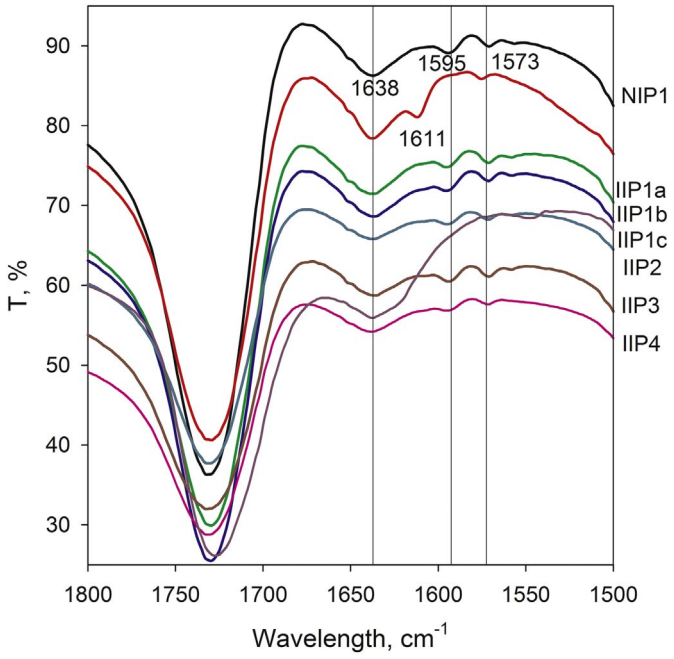

Fig. 5. FTIR spectra (KBr pellets) of NIP1, IIP1a containing nickel (before any acidic treatment), and all of the IIPs after H_2SO_4 regeneration.

5 M H_2SO_4 from IIPs containing 2-(aminomethyl)pyridine as the functional group [26]. The FTIR spectrum of the Vbamp monomer reveals stretching bands of C=C (from vinyl, benzene and pyridine) and C=N bands of pyridine at 1573, 1595 and 1638 cm^{-1} [26]. When amp forms a complex with nickel, the C=N stretching band is shifted from 1595 to 1611 cm^{-1} [35]. As an example, the spectrum of IIP1a containing nickel (before any acidic treatment) is compared to that of NIP1 and to all of the IIPs after H_2SO_4 regeneration (Fig. 5). This clearly shows that after regeneration using 5 M H_2SO_4, the shift of the C=N band from 1595 to 1611 cm^{-1} was no longer observed on the IIP spectra, thereby proving the decomplexation of nickel from the amp ligand and the leaching of the metal from the IIP matrix.

Nitrogen adsorption/desorption isotherms were measured for all NIPs (Fig. 6(A)) and IIPs (Fig. 6(B)). BET surface areas, pore volumes and average pore diameters calculated using the BJH model are shown in Table 3. The isotherm for NIP1 is of type IV with a hysteresis loop,

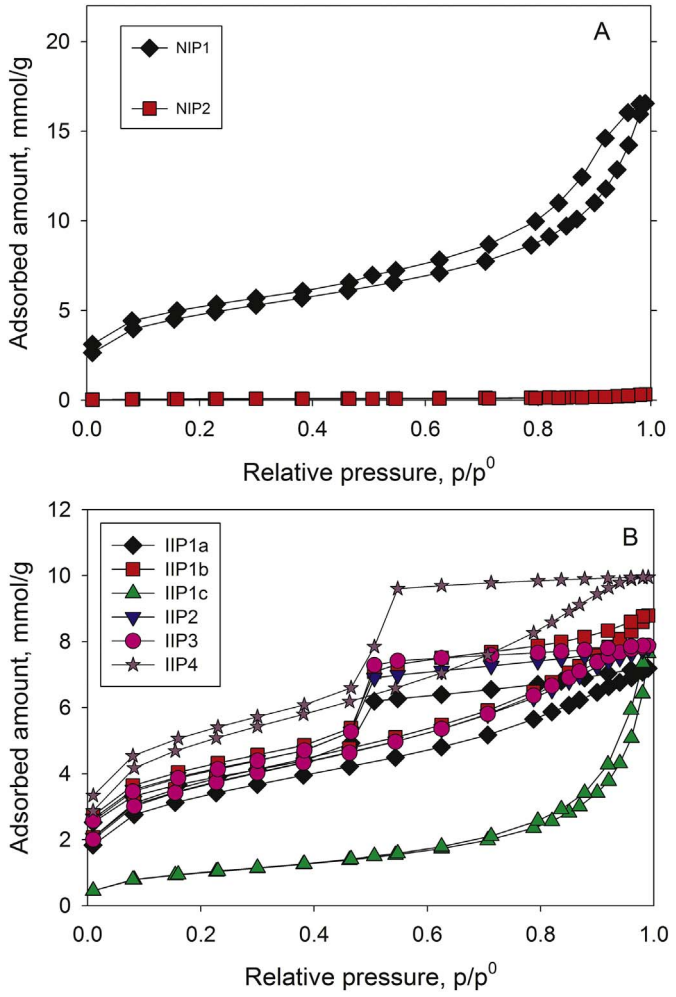

Fig. 6. Nitrogen adsorption/desorption isotherms of (A) NIP1 and NIP2, and (B) IIP1a, IIP1b, IIP1c, IIP2, IIP3, and IIP4 after acid-base pretreatment.

Table 3
Properties of NIPs and IIPs after acid-base pretreatment.

	NIP1	NIP2	IIP1a	IIP1b	IIP1c	IIP2	IIP3	IIP4
S_{BET} m^2/g	369	5.4	256	288	79.5	281	280	377
BJH porous volume, mL/g	0.49	–	0.19	0.24	0.25	0.21	0.21	0.25
Average pore diameter, nm	9.9	–	10	10	7.9	10.2	9.9	10.6
Nickel binding capacities, mmol/g, pH 4	0.048	0.003	0.033	0.060	0.011	0.04	0.064	0.059
Imprinting factor	–	–	0.7	1.3	0.3	12.4	1.3	1.2
k_{Zn}^{Ni}, -	754	110	1038	102	262	1441	1463	1402
k′	–	–	1.4	0.1	0.3	13	1.9	1.9

H1, which indicates a narrow distribution of independent mesopores [36]. The nitrogen adsorption/desorption isotherm for NIP2 shows very low adsorption and the BET surface is very small. This indicates a nonporous structure for NIP2.

In the case of the IIPs, only IIP1c exhibits an isotherm of type II with a hysteresis loop, H1, indicating a narrow distribution of independent macropores [36]. In the case of other IIPs (Fig. 6), type IV isotherms with H2 hysteresis loops indicate that their mesopores are interconnected and the distribution of pore size and the pore shape is ill-defined or irregular [36]. For those IIPs, BET surface areas, pore volumes and average pore diameters were also of the same magnitude. Structural properties for IIP3 and IIP4 were similar, meaning that the

proposed adjustment method for complex *in situ* formation yielded similar structural properties for IIP compared to IIP made by the conventional complex isolation method (crystallization, precipitation).

3.3. Metal binding properties of IIPs

Nickel loading, imprinting factors, selectivity coefficients for nickel over zinc and relative selectivity factors for NIPs and IIPs were studied at pH 4 (Table 3). This acidic pH value was chosen, because IIPs developed in this study are primarily developed for hydrometallurgical metal removal applications, in which solutions are usually acidic.

In order to study the effect of uncomplexed nickel on the properties of IIPs, IIPs of the [Ni(Vbamp)]$(NO_3)_2$ complex and three different amounts of uncomplexed nickel—9% (IIP1a), 33% (IIP1b) and 76% (IIP1c)—were studied. According to the results shown in Table 3, the nickel capacities of IIP1a and IIP1b are significantly higher than that of IIP1c. This is in accordance with the lower surface area of the IIP1c polymer. However, in the case of the nickel/zinc selectivity results, selectivity was high in the case in which the Ni/Vbamp ratio = 1.1 (IIP1a), but decreased significantly at Ni/Vbamp ratios = 1.5 (IIP1b) and 4.0 (IIP1c). Therefore, it was concluded that the amount of uncomplexed nickel during the polymerization should be below 10% in order not to affect the properties of the corresponding IIP.

The results of the effect of the stoichiometry of the complex on the nickel binding and selectivity properties of IIP1a, IIP2 and IIP3 are shown in Table 3. The nickel binding capacity increased as the stoichiometry of the complex changed from 1:1 to 1:3. One would assume the opposite result; however, one explanation may be that the higher the stoichiometry of the complex, the lower the stability constant of the acid. Nickel selectivity in the presence of zinc was high and independent of the stoichiometry of the complex. In the case of IIP1a, the selectivity coefficient is only slightly lower compared to IIP2 and IIP3. Furthermore, no significant differences between IIP2 and IIP3 were observed. The ion-imprinting factor for IIP2 was very high compared to the other complexes, because the corresponding NIP2 had a low nickel capacity attributed to its nonporous structure.

In order to evaluate the new adjustment method for forming the complexes, the properties of IIP3 were compared with those of IIP4 prepared with the $[Ni(Vbamp)_3]^{2+}$ complex, which was isolated prior to polymerization [31]. Despite a slight variation in the porous structures, all the binding, selectivity and imprinted characteristics of these two IIPs were almost equivalent, therefore proving that the method of isolating complexes described in the present paper is efficient and can be a very attractive alternative when the preparation of the complexes is difficult or impossible.

4. Conclusions

In this study, IIP complexes with three different stoichiometries—1:1, 1:2 and 1:3—between nickel and the *N*-(4-vinylbenzyl)-2-(aminomethyl)pyridine (Vbamp) monomer were adjusted by *in situ* complexation and polymerized by inverse suspension polymerization. An analogous IIP with the $[Ni(Vbamp)_3]^{2+}$ complex was synthesized also using precipitation as an isolation procedure in order to compare the effect of the two isolation methods on the properties of the IIPs. Additionally, the effect of uncomplexed nickel during the polymerization was investigated. Moreover, the significance of the isolation procedure in producing different stoichiometries and the effect of stoichiometry on separation material characteristics, including metal binding and selectivity properties, was elucidated.

According to the results, adjustment based on the Ni/Vbamp ratio succeeded well and all three complex structures $[Ni(Vbamp)]^{2+}$, $[Ni(Vbamp)_2]^{2+}$ and $[Ni(Vbamp)_3]^{2}$ could be formed selectively *in situ*. The amount of uncomplexed nickel during the polymerization should be below 10% of the total nickel concentration in order to avoid a negative influence on the properties of the IIPs. When the complex stoichiometry is changing from 1:1 to 1:3 complex stoichiometry selectivity coefficients are increasing significantly. However, the difference between the selectivity coefficients of the 1:2 and 1:3 complex stoichiometries was not significant. Results clearly showed that structural properties, metal binding abilities and selectivity properties of the IIPs were comparable with both isolation methods.

From a more general point of view, the results of this study are stepforward in IIPs development. As complex adjustment can be quite easily performed, it simplifies IIPs preparation process when complicated complex isolation methods (crystallization, precipitation) are not possible or necessary. Furthermore, IIPs selectivity is also dependent on the solvent used in the polymerization. This work gives therefore more options to adapt the solvents because redissolution of isolated complexes is not problematic anymore. The only limitation is that this method is only suitable for the complexes which can be detected by UV–vis spectrophotometer.

Acknowledgments

This work was financially supported by the Academy of Finland, the Research Foundation of the Lappeenranta University of Technology, the Magnus Ehrnrooth Foundation and the Finnish Cultural Foundation. South Karelia Regional Funds are gratefully acknowledged. The authors are thankful to D.Sc. Tuomas Sihvonen and Ms. Anne Hyrkkänen for assistance with the experimental and analytical work.

References

[1] T.P. Rao, S. Daniel, J. Mary Gladis, Tailored materials for preconcentration or separation of metals by ion-imprinted polymers for solid-phase extraction (IIP-SPE), TrAC Trends Anal. Chem. 23 (2004) 28–35.
[2] Ö. Saatçılar, N. Satıroglu, R. Say, S. Bektas, A. Denizli, Binding behavior of Fe^{3+} ions on ion-imprinted polymeric beads for analytical applications, J. Appl. Polym. Sci. 101 (2006) 3520–3528.
[3] C. Branger, W. Meouche, A. Margaillan, Recent advances on ion-imprinted polymers, React. Funct. Polym. 73 (2013) 859–875.
[4] A.E. Martell, R.D. Hancock, Metal Complexes in Aqueous Solutions, Plenum Press, New York, 1996.
[5] J. Fu, L. Chen, J. Li, Z. Zhang, Current status and challenges of ion imprinting, J. Mater. Chem. A 3 (2015) 13598–13627.
[6] A. Bhaskarapillai, S.V. Narasimhan, A comparative investigation of copper and cobalt imprinted polymers: evidence for retention of the solution-state metal ion–ligand complex stoichiometry in the imprinted cavities, RSC Adv. 3 (2013) 13178–13182.
[7] A. Bhaskarapillai, N.V. Sevilimedu, B. Sellergren, Synthesis and characterization of imprinted polymers for radioactive waste reduction, Ind. Eng. Chem. Res. 48 (2009) 3730–3737.
[8] E. Birlik, A. Ersöz, E. Acıkkalp, A. Denizli, R. Say, Cr(III)-imprinted polymeric beads: sorption and preconcentration studies, J. Hazard. Mater. 140 (2007) 110–116.
[9] A.H. Dam, D. Kim, Metal ion-imprinted polymer microspheres derived from copper methacrylate for selective separation of heavy metal ions, J. Appl. Polym. Sci. 108 (2008) 14–24.
[10] M. Firouzzare, Q. Wang, Synthesis and characterization of a high selective mercury (II)-imprinted polymer using novel aminothiol monomer, Talanta 101 (2012) 261–266.
[11] H.R. Rajabi, S. Razmpour, Synthesis, characterization and application of ion imprinted polymeric nanobeads for highly selective preconcentration and spectrophotometric determination of Ni^{2+} ion in water samples, Spectrochim. Acta A Mol. Biomol. Spectrosc. 153 (2016) 45–52.
[12] M. Saraji, H. Yousefi, Selective solid-phase extraction of Ni(II) by an ion-imprinted polymer from water samples, J. Hazard. Mater. 167 (2009) 1152–1157.
[13] D.K. Singh, S. Mishra, Synthesis, characterization and analytical applications of Ni (II)-ion imprinted polymer, Appl. Surf. Sci. 256 (2010) 7632–7637.
[14] J. Otero-Romaní, A. Moreda-Pineiro, P. Bermejo-Barrera, A. Martin-Esteban, Synthesis, characterization and evaluation of ionic-imprinted polymers for solid-phase extraction of nickel from seawater, Anal. Chim. Acta 630 (2008) 1–9.
[15] S. Chaitidou, O. Kotrotsiou, C. Kiparissides, On the synthesis and rebinding properties of $[Co(C_2H_3O_2)_2$(z-Histidine)] imprinted polymers prepared by precipitation polymerization, Mater. Sci. Eng. C 29 (2009) 1415–1421.
[16] M. Shamsipur, J. Fasihi, A. Khanchi, R. Hassani, K. Alizadeh, H.A. Shamsipur, A stoichiometric imprinted chelating resin for selective recognition of copper(II) ions in aqueous media, Anal. Chim. Acta 599 (2007) 294–301.
[17] M. Shamsipur, A. Besharati-Seidani, J. Fasihi, H. Sharghi, Synthesis and characterization of novel ion-imprinted polymeric nanoparticles for very fast and highly selective recognition of copper(II) ions, Talanta 83 (2010) 674–681.
[18] B. Gao, F. An, Y. Zhu, Novel surface ionic imprinting materials prepared via couple

grafting of polymer and ionic imprinting on surfaces of silica gel particles, Polymer 48 (2007) 2288–2297.
[19] B. Gao, F. An, K. Liu, Studies on chelating adsorption properties of novel composite material polyethyleneimine/silica gel for heavy-metal ions, Appl. Surf. Sci. 253 (2006) 1946–1952.
[20] J. Fasihi, S. Ammari Alahyari, M. Shamsipur, H. Sharghi, A. Charkhi, Adsorption of uranyl ion onto an anthraquinone based ion-imprinted copolymer, React. Funct. Polym. 71 (2011) 803–808.
[21] S. Daniel, P. Prabhakara Rao, T. Prasada Rao, Investigation of different polymerization methods on the analytical performance of palladium(II) ion imprinted polymer materials, Anal. Chim. Acta 536 (2005) 197–206.
[22] J. Fu, X. Wang, J. Li, Y. Dinga, L. Chen, Synthesis of multi-ion imprinted polymers based on dithizone chelation for simultaneous removal of Hg^{2+}, Cd^{2+}, Ni^{2+} and Cu^{2+} from aqueous solutions, RSC Adv. 6 (2016) 44087–44095.
[23] P. Job, Formation and stability of inorganic complexes in solution, Ann. Chim. 9 (1928) 113–203.
[24] P. Gans, A. Sabatini, A. Vacca, SUPERQUAD: an improved general program for computation of formation constants from potentiometric data, J. Chem. Soc. Dalton Trans. (1985) 1195–1200.
[25] M. Laatikainen, K. Laatikainen, S.-P. Reinikainen, H. Hyvönen, C. Branger, H. Siren, T. Sainio, Complexation of nickel with 2-(aminomethyl)pyridine at high zinc concentrations or in non-aqueous solvent mixture, J. Chem. Eng. Data 59 (2014) 2207–2214.
[26] K. Laatikainen, D. Udomsap, H. Sirén, H. Brisset, T. Sainio, C. Branger, Effect of template ion-ligand complex stoichiometry on selectivity of ion-imprinted polymers, Talanta 134 (2015) 538–545.
[27] V. Lenoble, K. Laatikainen, C. Garnier, B. Angeletti, B. Coulomb, T. Sainio, C. Branger, Nickel retention by an ion-imprinted polymer: wide-range selectivity study and modelling of the binding structures, Chem. Eng. J. 304 (2016) 20–28.
[28] X. Cai, J. Li, Z. Zhang, F. Yang, R. Dong, L. Chen, Novel Pb^{2+} ion imprinted polymers based on ionic interaction via synergy of dual functional monomers for selective solid-phase extraction of Pb^{2+} in water samples, ACS Appl. Mater. Interfaces 6 (2014) 305– − 313.
[29] Z. Zhang, J. Li, X. Song, J. Ma, L. Chen, Hg^{2+} ion-imprinted polymers sorbents based on dithizone–Hg^{2+} chelation for mercury speciation analysis in environmental and biological samples, RSC Adv. 4 (2014) 46444–46453.
[30] S. Xu, L. Chen, J. Li, Y. Guan, H. Lu, Novel Hg^{2+}-imprinted polymers based on thymine–Hg^{2+}–thymine interaction for highly selective preconcentration of Hg^{2+} in water samples, J. Hazard. Mater. 237–238 (2012) 347–354.
[31] E. Garcia-Espana, F. Nuzzi, A. Sabatini, A. Vacca, Reactions of 2-(aminomethyl) pyridine with hydrogen-ion and divalent transition-metal ions. 1. Equilibrium-constants, Gazz. Chim. Ital. 115 (1985) 607–611.
[32] S. Dai, M.C. Burleig, Y. Shin, C.C. Morrow, C.E. Barnes, Z. Xue, A Imprint coating: a novel synthesis of selective functionalized ordered mesoporous sorbents, Angew. Chem. Int. Ed. Engl. 38 (1999) 1235–1239.
[33] S. Tanase, M. Ferbinteanu, M. Andruh, C. Mathoniére, I. Strenger, G. Rombaut, Synthesis and characterization of a new molecular magnet, $[Ni(ampy)_2]_3[Fe(CN)_6]_2{\cdot}6H_2O$ and synthesis, crystal structure and magnetic properties of its mononuclear precursor, *trans*-$[Ni(ampy)_2(NO_3)_2]$ (ampy-2-aminomethylpyridine), Polyhedron 19 (2000) 1967–1973.
[34] W. Meouche, C. Branger, I. Beurroies, R. Denoyel, A. Margaillan, Inverse suspension polymerization as a new tool for the synthesis of ion-imprinted polymers, Macromol. Rapid Commun. 33 (2012) 928–932.
[35] S. Bruda, M.M. Turnbull, C.P. Landee, Q. Xu, Synthesis, structures and magnetic properties of 2-aminomethylpyridine–Ni(II) complexes, Inorg. Chim. Acta 359 (2006) 298–308.
[36] K.S.W. Sing, D.H. Everett, R.A.W. Haul, L. Moscou, R.A. Pierotti, J. Rouquerol, Physical biophysical chemistry division commission on colloid and surface chemistry including catalysis, Pure Appl. Chem. 57 (1985) 603–619.